experiments, in each case adding 0.23 Sv to the local surface freshwater flux over 1,500 yr and 'tagging' the melt water with a $\delta^{18}O$ value of $-40‰$ (the background $\delta^{18}O$ value is assumed zero everywhere). The model offers insight into the likely spatial and depth-dependent distributions of meltwater-induced $\delta^{18}O$ anomalies, while accounting for the impacts of ocean dynamics on the result. Sensitivity tests have been undertaken with $\delta^{18}O$ values of $-30‰$ and $-50‰$. The main experiments considered a series of different meltwater release scenarios: 100% in the North Atlantic zone 50–70° N (additional experiments considered partial or complete release into the Gulf of Mexico); a 50:50 split between the North Atlantic and around Antarctica; 100% around Antarctica; and 20:80, 30:70 and 40:60 splits between the North Atlantic and Antarctica. For diagnostic purposes we averaged $\delta^{18}O$ over four major basins (Atlantic, Southern Ocean, Pacific, Indian) in four layers (upper, 0–411 m; intermediate, 411–1,158 m; deep, 1,158–2,520 m; bottom, 2,520–5,000 m).

The model has a simplified atmosphere, no carbon cycle (that is, no $CO_2$ and $CH_4$ feedbacks), no interactive ice sheets and no insolation changes or solar variability. The scenarios presented are part of a suite of experiments in which the proportions between North Atlantic and Antarctic meltwater combinations were varied in 10% increments. The scenarios comprise constant and simultaneous meltwater fluxes into the North Atlantic and (equally distributed) around Antarctica. As part of the sensitivity analyses, some scenarios have also been run with differently phased northern and southern inputs. In total, nearly 150 4,000-yr simulations have been performed to ensure that the results discussed in this paper are robust with regard to all feasible combinations for the key model parameters.

In the EMIC, the Atlantic overturning is very sensitive to the location of imposed meltwater releases, similarly to previous studies[17,29,30]. In our extreme case with 100% meltwater release into the North Atlantic, the Atlantic overturning circulation collapses rapidly (Fig. 2), preserving a strong local $\delta^{18}O$ signal in surface layers during, and shortly after, the period of freshwater release (Fig. 3a). The same collapse (and corresponding isotopic signal) is obtained with every combination of key model parameters considered here (Supplementary Fig. 4). Similar tests for robustness have been made for the 50:50, 40:60 and 30:70 scenarios. These experiments confirm the robustness of our main results, namely the collapse of Atlantic overturning under a sustained local freshwater flux anomaly of about 0.1 Sv, in agreement with other studies[29,30].

1. Langway, C. C. Jr, Oeschger, H. & Dansgaard, W. (eds) *Greenland Ice Core: Geophysics, Geochemistry, and the Environment* (Geophys. Monogr. 33, Am. Geophys. Union, Washington DC, 1985).
2. Grootes, P. M., Stuiver, M., White, J. W. C., Johnsen, S. & Jouzel, J. Comparison of oxygen isotope records from the GISP2 and GRIP Greenland ice cores. *Nature* **366**, 552–554 (1993).
3. Dansgaard, W. *et al.* Evidence for general instability of past climate from a 250 kyr ice core. *Nature* **364**, 218–219 (1993).
4. Rahmstorf, S. Timing of abrupt climate change: a precise clock. *Geophys. Res. Lett.* **30** doi:10.1029/2003GL017115 (2003).
5. Broecker, W. S. Abrupt climate change: causal constraints provided by the paleoclimate record. *Earth Sci. Rev.* **51**, 137–154 (2000).
6. Voelker, A. H. *et al.* Global distribution of centennial-scale records for marine isotope stage (MIS) 3: a database. *Quat. Sci. Rev.* **21**, 1185–1212 (2002).
7. Leuschner, D. C. & Sirocko, F. The low-latitude monsoon climate during Dansgaard–Oeschger cycles and Heinrich events. *Quat. Sci. Rev.* **19**, 243–254 (2000).
8. Rohling, E. J., Mayewski, P. A. & Challenor, P. On the timing and mechanism of millennial-scale climate variability during the last glacial cycle. *Clim. Dyn.* **20**, 257–267 (2003).
9. Pahnke, K., Zahn, R., Elderfield, H. & Schultz, M. 340,000-year centennial-scale marine record of Southern Hemisphere climatic oscillation. *Science* **301**, 948–952 (2003).
10. Blunier, T. *et al.* Asynchrony of Antarctic and Greenland climate change during the last glacial period. *Nature* **394**, 739–743 (1998).
11. Hemming, S. R. Heinrich events: Massive detritus layers of the North Atlantic and their global climate impact. *Rev. Geophys.* **42**, RG1005, doi: 10.1029/2003RG 000128 (2004).
12. Shackleton, N. J., Hall, M. A. & Vincent, E. Phase relationships between millennial-scale events 64,000–24,000 years ago. *Paleoceanography* **15**, 565–569 (2000).
13. Siddall, M. *et al.* Sea-level fluctuations during the last glacial cycle. *Nature* **423**, 853–858 (2003).
14. Cutler, K. B. *et al.* Rapid sea-level fall and deep-ocean temperature change since the last interglacial period. *Earth Planet. Sci. Lett.* **206**, 253–271 (2003).
15. Kanfoush, S. L. *et al.* Millennial-scale instability of the Antarctic ice sheet during the last glaciation. *Science* **288**, 1815–1818 (2000).
16. Clark, P. U., Mitrovica, J. X., Milne, G. A. & Tamisiea Sea-level fingerprinting as a direct test for the source of global meltwater pulse 1A. *Science* **295**, 2438–2441 (2002).
17. Weaver, A. J., Saenko, O. A., Clark, P. U. & Mitrovica, J. X. Meltwater pulse 1A from Antarctica as a trigger for the Bølling-Allerød warm interval. *Science* **299**, 1709–1713 (2003).
18. Stocker, T. F. & Johnsen, S. J. A minimum thermodynamic model for the bipolar seesaw. *Paleoceanography* **18**, PA1087, doi:10.1029/2003PA000920 (2003).
19. Ganopolski, A. & Rahmstorf, S. Rapid changes of glacial climate simulated in a coupled climate model. *Nature* **409**, 153–158 (2001).
20. Barrett, P. J. Antarctic palaeoenvironment through Cenozoic times—a review. *Terra Antartica* **3**, 103–119 (1996).
21. Peltier, W. R. Ice Age palaeotopography. *Science* **265**, 195–201 (1994).
22. Huybrechts, P. Sea-level changes at the LGM from ice-dynamic reconstructions of the Greenland and Antarctic ice sheets during the glacial cycles. *Quat. Sci. Rev.* **21**, 203–231 (2002).
23. Denton, G. H. & Hughes, T. J. Reconstructing the Antarctic Ice Sheet at the Last Glacial Maximum. *Quat. Sci. Rev.* **21**, 193–202 (2002).
24. Anderson, J. B., Shipp, S. S., Lowe, A. L., Wellner, J. S. & Mosola, A. B. The Antarctic Ice Sheet during the Last Glacial Maximum and its subsequent retreat history: a review. *Quat. Sci. Rev.* **21**, 49–70 (2002).
25. Annan, J. D., Hargreaves, J. C., Edwards, N. R. & Marsh, R. Parameter estimation in an intermediate complexity earth system model using an ensemble Kalman filter. *Ocean Model.* (in the press).
26. Edwards, N. R. & Marsh, R. Uncertainties due to transport parameter sensitivity in an efficient 3-D ocean-climate model. *Clim. Dyn.* (submitted) (2004).
27. Stenni, B. *et al.* A late-glacial high-resolution site and source temperature record derived from the EPICA Dome C isotope records (East Antarctica). *Earth Planet. Sci. Lett.* **217**, 183–195 (2003).
28. Indermühle, A., Monnin, E., Stauffer, B., Stocker, T. F. & Wahlen, M. Atmospheric $CO_2$ concentration from 60 to 20 kyr BP from the Taylor Dome ice core, Antarctica. *Geophys. Res. Lett.* **27**, 735–738 (1999).
29. Rahmstorf, S. Bifurcations of the Atlantic thermohaline circulation in response to changes in the hydrological cycles. *Nature* **378**, 145–149 (1995).
30. Rahmstorf, S. Rapid climate transitions in a coupled ocean–atmosphere model. *Nature* **372**, 82–85 (1994).

··············································································

# A Middle Jurassic 'sphenosuchian' from China and the origin of the crocodylian skull

**James M. Clark**[1], **Xing Xu**[2]*, **Catherine A. Forster**[3] & **Yuan Wang**[2]

[1]*Department of Biological Sciences, George Washington University, Washington DC 20052, USA*
[2]*Institute of Vertebrate Paleontology and Paleoanthropology, Chinese Academy of Sciences, 142 Xiwai Street, Beijing, 100044, China*
[3]*Department of Anatomical Sciences, Stony Brook University, Stony Brook, New York 11794, USA*

* Present address: Department of Paleontology, American Museum of Natural History, 79th Street at Central Park West, New York 10024, USA

....................................................................................

**The skull of living crocodylians is highly solidified and the jaw closing muscles are enlarged[1], allowing for prey capture by prolonged crushing between the jaws. Living species are all semi-aquatic, with sprawling limbs and a broad body that moves mainly from side-to-side[2]; however, fossils indicate that they evolved from terrestrial forms. The most cursorial of these fossils[3–6] are small, gracile forms often grouped together as the Sphenosuchia, with fully erect, slender limbs; their relationships, however, are poorly understood[5,7–10]. A new crocodylomorph from deposits in northwestern China of the poorly known Middle Jurassic epoch possesses a skull with several adaptations typical of living crocodylians. Postcranially it is similar to sphenosuchians but with even greater adaptations for cursoriality in the forelimb. Here we show, through phylogenetic analysis, that it is the closest relative of the large group Crocodyliformes, including living crocodylians. Thus, important features of the modern crocodylian skull evolved during a phase when the postcranial skeleton was evolving towards greater cursoriality, rather than towards their current semi-aquatic habitus.**

The Sphenosuchia includes nine monotypic genera comprising the most basal members of the Crocodylomorpha, but its monophyly has been controversial. Sphenosuchians were once[7] thought to be a paraphyletic assemblage with some taxa closer to the large group Crocodyliformes. Later evidence suggested that Sphenosuchia is a monophyletic group[5,8–10], but some analyses found no resolution owing to conflicting data[6]. Members of the Crocodyliformes are diagnosed by a large suite of features[11], some of which are related to the solidifying of intracranial joints and an increase in the

size of muscles responsible for producing a powerful bite force. The new taxon possesses several of these features and greatly reduces the morphological gap between sphenosuchians and crocodyliforms.

Sphenosuchians are found on every continent except Antarctica and Australasia and in deposits from the Late Triassic to the Early Jurassic, and possibly the Late Jurassic[6,12]. These small (<1.5 m total length) animals are among the most gracile of non-flying archosaurs. The hindlimb is known in several sphenosuchian taxa in which its morphology indicates that it moved within a vertical, parasagittal plane[3,4]; however, the forelimb and the axial skeleton are not as well known or studied. The new specimen, comprising the

front half of a skeleton, was discovered during recent fieldwork that we directed at Wucaiwan, Xinjiang[13]. It is the most complete skeleton of a non-marine crocodylomorph from the Middle Jurassic.

The skeleton possesses four features typical of the large group Crocodylomorpha[6,9,10]: a broad squamosal overhanging the temporal region; a medially shifted quadrate contacting the lateral surface of the braincase; a ventrally elongate coracoid; and an elongate radiale and ulnare. It includes typical sphenosuchian features[9,10] such as the thin, ventrally concave squamosal with a curved posterolateral edge, a compact carpus and a posteroventrally curving rod-like ventral process of the coracoid. Although it lacks most features diagnostic of the Crocodyliformes[11]—a heavily sculptured skull, a shorter rostrum, a flat skull roof, a smaller antorbital fossa and fenestra, and an anteroposteriorly expanded ventral end of the coracoid—it possesses several features previously not found in sphenosuchians.

Our phylogenetic analysis places *Junggarsuchus* as the sister-group of crocodyliforms, identifying five unambiguous synapomorphies (Fig. 1). Of trees that are two steps longer than ours, some have a monophyletic Sphenosuchia including *Junggarsuchus*, and bootstrap support for the *Junggarsuchus*-crocodyliform node is 61%. Unambiguous synapomorphies, identified by our phylogenetic analysis, include the following (character numbers in brackets are from the phylogenetic analysis, see Supplementary Information): (20) exoccipitals meet on the midline above the foramen magnum; (36) the large ventrolateral extension of the exoccipital contacts the quadrate; (37) the jugal is strongly arched dorsally; (42) the occipital portion of the parietal is narrow; and (46) the quadrate is fenestrated. *Dibothosuchus* (7, 22, 41) and *Sphenosuchus* (16, 19) are nested with this group on the basis of the following unambiguous synapomorphies, all from the skull: (7) the prefrontal does not underlie the frontal; (22) the mastoid antrum enters deeply into the prootic; (41) a horizontal shelf in the posterior part of the supratemporal fenestra; (16) the parietals are fused; and (19) the occipital margin is straight.
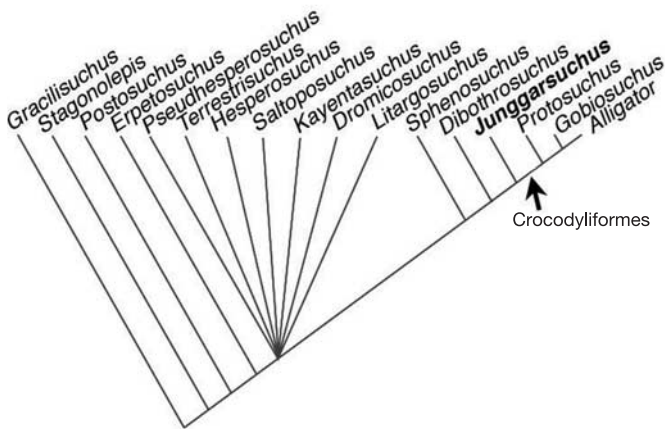


**Figure 1** Results of a maximum parsimony phylogenetic analysis. Strict consensus of 81 trees; length = 109, consistency index (CI) = 0.569, retention index (RI) = 0.659. *Junggarsuchus* is the closest relative of the Crocodyliformes and the Sphenosuchia are paraphyletic. See Supplementary Information for details of the analysis.
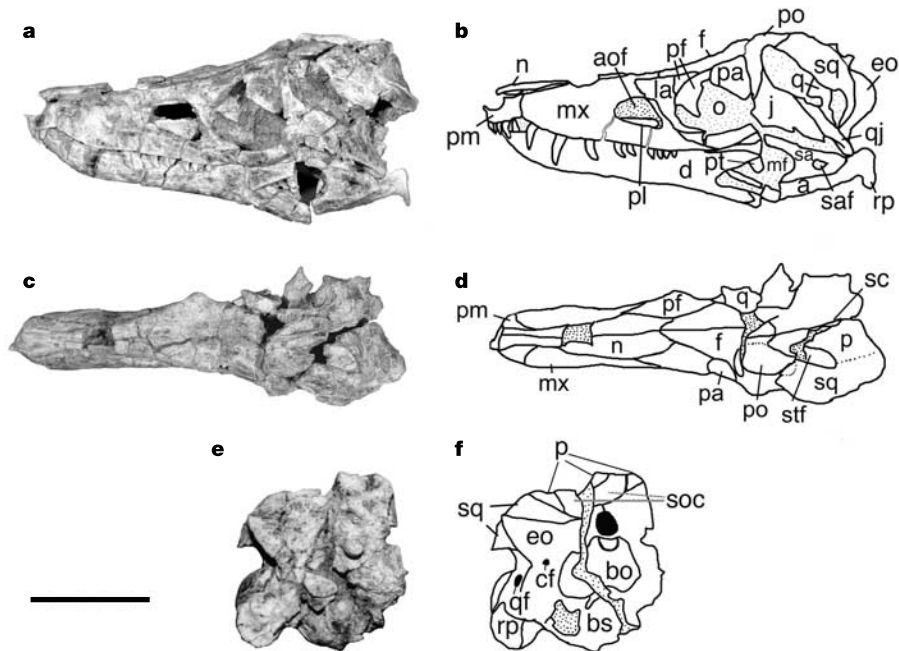


**Figure 2** *Junggarsuchus sloani* holotype skull. **a**, **b**, Left lateral view. **c**, **d**, Dorsal view. **e**, **f**, Occipital view. a, angular; aof, antorbital fenestra; bo, basioccipital; bs, basisphenoid; cf, carotid foramen; d, dentary; eo, exoccipital; f, frontal; j, jugal; la, lacrimal; mf, external mandibular fenestra; mx, maxilla; n, nasal; o, orbit; p, parietal; pa, palpebral; pf, prefrontal; pl, palatine; pm, premaxilla; po, postorbital; pt, pterygoid; q, quadrate; qf, quadrate fenestra; qj, quadratojugal; rp, retroarticular process; sa, surangular; saf, surangular foramen; sc, sagittal crest; soc, supraoccipital; sq, squamosal; stf, superior temporal fenestra. Scale bar, 5 cm.

The skull (Fig. 2) is notable for its lack of kinesis and the reduction in the supratemporal fenestrae, as in crocodyliforms. A ventrolateral extension of the otoccipital connects with the distal end of the quadrate, solidifying the temporal region and preventing any movement of the quadrate. Broadened areas for muscle attachment on the arched jugal and surangular indicate an increased size of the Musculus adductor mandibulae externus pars superficialis. As in living crocodylians, but not the most basal crocodyliforms or sphenosuchians, the lateral surface of the angular has a large area for the insertion of the M. pterygoideus posterior extending onto the anterolateral surface of the retroarticular process.

Procoelous vertebral joints, a lack of osteoderms, and trunk vertebrae with short transverse processes and sub-vertical zygapophyses indicate that the body had a greater capacity for vertical movement than in living crocodylians. The lack of osteoderms on the specimen is unlikely to be due to taphonomic loss or ontogenetic immaturity because the rest of the skeleton is preserved undisturbed and the fusion of neurocentral sutures indicates adulthood[14]. In living crocodylians the osteoderms are tightly



**Figure 3** Postcranial skeleton of *Junggarsuchus sloani*. **a**, Skeleton in left lateral view. **b**, Left humerus with hemispherical head in proximal view. **c**, Posteroventrally facing glenoid fossa of left scapula in distal view. **d**, Left carpus and manus in posteroventral view (arrow points to reduced fifth metacarpal). **e**, **f**, For comparison, the living *Alligator mississippiensis* left humerus and shoulder in lateral view (**e**) showing the hemi-sellar glenoid fossa, and left hand in dorsal view (**f**) showing the asymmetry of the digits and carpals, the rounded ulna–carpal contact (arrow) and the single distal carpal (stippled area is cartilaginous). dc, distal carpal; g, glenoid fossa; h, humerus; hh, head of humerus; hyp, hypapophyses; ra, radius; rl, radiale; sc, scapula; ue, ulnare; ul, ulna; I–V, digits of hand. **f** was modified from ref. 16. Scale bars, 4 cm (**a**) and 1 cm (**b–d**).

bound to the axial skeleton through tendinous connections to large epaxial muscles originating on long transverse processes[2]. Together with the nearly horizontal zygapophyseal articulations of the dorsal vertebrae this system greatly restricts vertical mobility and facilitates undulating lateral movements. *Junggarsuchus* vertebrae in the anterior trunk and shoulder regions have small or no transverse processes, and zygapophyses that are oriented less than 30 degrees from the vertical (Fig. 3).
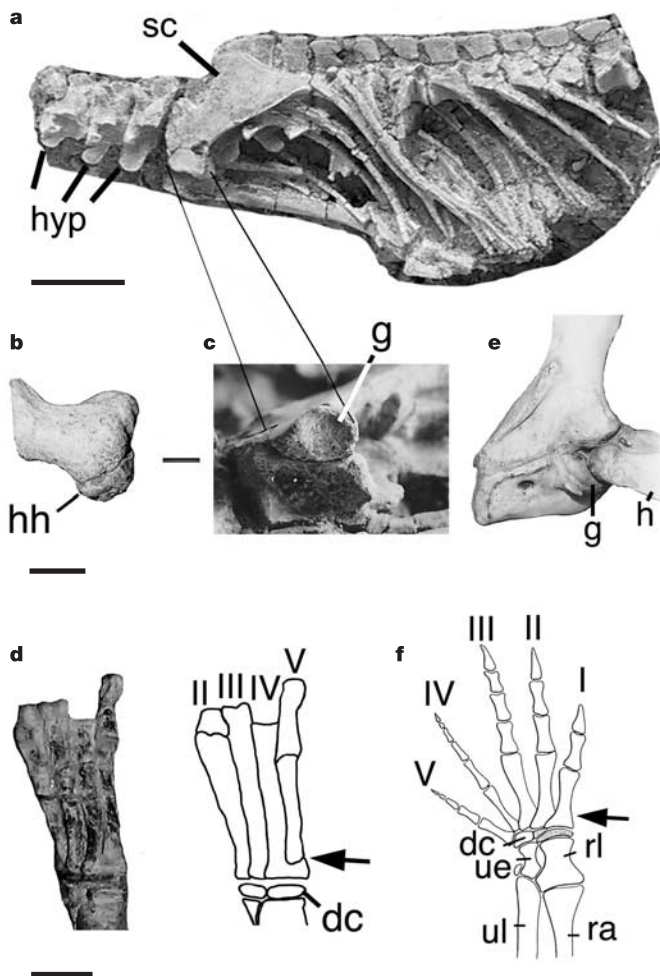
The configuration of the shoulder and wrist and the reduction of the outer fingers indicate that the forelimb was held directly beneath the body. In living crocodylians the shoulder joint involves a posterolaterally facing, notch-shaped glenoid fossa and an elongate, convex humeral head (Fig. 3). This 'hemi-sellar' type of joint is present in all living amniotes except mammals[15]. The glenoid fossa of *Junggarsuchus* instead involves a ventrally or posteroventrally facing concave scapular component superficially similar to that of mammals and a smaller, posteriorly facing much shallower coracoid component. The humerus of *Junggarsuchus* is unlike that of any other crocodylomorph in that it has a well-developed hemispherical head projecting perpendicular to the shaft, with a convex proximal articulating surface. The convex head must have articulated with the concave scapular glenoid fossa and have been buttressed anteriorly by the coracoid, so that the shaft of the humerus was vertical or posteroventrally inclined.

The wrist indicates that movement of the hand was in line with the rest of the forelimb and not splayed out as in living crocodylians. In living crocodylians the wrist forms a complex joint in which the broadly convex distal end of the ulna articulates with both proximal carpal bones, which rotate against the ulna when walking, spreading the hand. In *Junggarsuchus* the distal end of the ulna is squared off, and the contact for the radiale on the medial side of the ulna is perpendicular to the rounded distal articulation surface with the ulnare, limiting rotation against the ulna. In living crocodylians there is only one distal carpal and it lies laterally so that the carpal–metacarpal joint is oblique[16]; in *Junggarsuchus* the two distal carpals are flattened, equally thick and form a straight joint perpendicular to the long axes of the radiale and ulnare.

The first digit is absent and the fifth digit was relatively small, flexing towards the other toes rather than facing the ground, making the hand functionally tridactyl. In living crocodylians the five fingers are usually spread out lateral to the forearm during locomotion and all face the ground. The first three digits are robust and the other two are smaller. In *Junggarsuchus* the four metacarpals are like those of sphenosuchians in that they are compressed together proximally and not spread out[5,9], suggesting the manus was digitigrade. Metacarpal V is about half the thickness of metacarpals II–IV and shortened proximally so that it does not reach the carpus. The distal articulating surface of metacarpal V is oriented such that the phalanx flexes towards the other digits rather than posteroventrally, and the metacarpal joint surface is not ginglymoid like those of II–IV. Metacarpal IV is similar in size to metacarpal II, so that the metacarpals of the three weight-bearing digits (II–IV) are symmetrical in size.

The orientation of the glenoid fossa, the convex head on the humerus, the lack of rotation around the distal end of the ulna, the compact metacarpals and reduced outer digits all indicate that the limb moved in a vertical, parasagittal plane. Reduction of the outer digits is typical of highly cursorial mammals[17].

The paraphyly of sphenosuchians implies that the postcranial features shared among these taxa are ancestral for crocodyliforms rather than specializations of 'Sphenosuchia'. The posteroventrally oriented, concave glenoid fossa on the scapula, the elongate process on the coracoid, the compact carpus and the extremely slender limbs were gained in sphenosuchians and then lost in crocodyliforms. The 'Sphenosuchia' was thus a phase in the evolution of crocodylomorphs during which the group as a whole became highly adapted for terrestriality. The procoelous vertebrae, lack of osteo-

©2004 **Nature Publishing Group**

# letters to nature

derms, inturned humeral head and reduced digits of *Junggarsuchus* indicate that the closest known relative of crocodyliforms was also the most highly adapted cursor. The consolidation of the crocodylian skull thus began well before crocodylians entered the water. ☐

## Methods

Order Crocodylomorpha Hay, 1930 *sensu* Walker, 1970[3]
**Junggarsuchus sloani** gen. et sp. nov.

**Etymology.** For the Junggar Basin in northern Xinjiang, *souchous* (Greek) meaning crocodile and for C. Sloan, who discovered the holotype.

**Holotype.** IVPP V14010, (Institute of Vertebrate Paleontology and Paleoanthropology, Beijing), the articulated anterior half of a skeleton including a nearly complete skull (Figs 2 and 3).

**Locality and age.** Lower part of the Shishugou Formation[18] at Wucaiwan, Altay Prefecture, Xinjiang. The lower Shishugou (also known as the Wucaiwan Formation) is considered late Middle Jurassic (Bathonian–Callovian)[19,20].

**Diagnosis.** Small (body length ~1 m) non-crocodyliform crocodylomorph with longitudinal concavity on ventrolateral surface of dorsally arched jugal, broadened dorsal edge of surangular, shallow fossa on distal edge of paroccipital process and part of squamosal, enlarged anterior maxillary teeth, well developed surangular foramen, retroarticular process lacking medial process and with broad dorsolateral and posteroventral flanges, shallow procoely in all preserved vertebrae, anteroposteriorly and distally elongate hypapophyses on posterior 4 cervical and anterior 4 dorsal vertebrae, broadened posterior border and sinusoidal dorsal edge on scapula, anteriorly directed humeral head and reduced deltopectoral crest, reduced metacarpal V not contacting carpus, no manus digit I, and no osteoderms.

## Phylogenetic analysis

Phylogenetic relationships were analysed using a matrix of 55 characters from the skull and postcranial skeleton distributed among 17 taxa (see Supplementary Information). The taxa included four outgroups and three representatives of the Crocodyliformes. The matrix is derived from earlier studies[10] with 16 additional characters and the addition of *Junggarsuchus*, *Erpetosuchus*[21] and *Gobiosuchus*[22]. The data were analysed in PAUP*[23].

Received 20 May; accepted 2 July 2004; doi:10.1038/nature02802.

1. Iordansky, N. N. in *Biology of the Reptilia* (eds Gans, C. & Parsons, T. S.) **Vol. 4** 201–262 (Academic, New York, 1973).
2. Salisbury, S. W. & Frey, E. in *Crocodilian Biology and Evolution* (eds Grigg, G. C., Seebacher, F. & Franklin, C. E.) 85–134 (Surrey Beatty and Sons, Chipping Norton, Australia, 2001).
3. Walker, A. D. A revision of the Jurassic reptile *Hallopus victor* (Marsh), with remarks on the classification of crocodiles. *Phil. Trans. R. Soc. Lond. B* **257**, 323–372 (1970).
4. Parrish, J. M. The origin of crocodylian locomotion. *Paleobiol.* **13**, 396–414 (1987).
5. Sereno, P. C. & Wild, R. *Procompsognathus*: theropod, 'thecodont' or both? *J. Vert. Paleontol.* **12**, 435–458 (1992).
6. Clark, J. M. & Sues, H.-D. Two new species of basal crocodylomorphs and the status of the Sphenosuchia. *Zool. J. Linn. Soc.* **136**, 77–96 (2002).
7. Benton, M. J. & Clark, J. M. in *The Phylogeny and Classification of the Tetrapods* (ed. Benton, M. J.) Vol. 1 295–338 (Clarendon, London, 1988).
8. Wu, X.-C. & Chatterjee, S. *Dibothrosuchus elaphros*, a crocodylomorph from the Lower Jurassic of China and the phylogeny of the Sphenosuchia. *J. Vert. Paleontol.* **13**, 58–89 (1993).
9. Clark, J. M., Sues, H.-D. & Berman, D. S. A new specimen of *Hesperosuchus agilis* from the Upper Triassic of New Mexico and the interrelationships of basal crocodylomorph archosaurs. *J. Vert. Paleontol.* **20**, 683–704 (2001).
10. Sues, H.-D., Olsen, P. E., Carter, J. G. & Scott, D. M. A new crocodylomorph archosaur from the Upper Triassic of North Carolina. *J. Vert. Paleontol.* **23**, 329–343 (2003).
11. Clark, J. M. in *In the Shadow of the Dinosaurs: Early Mesozoic Tetrapods* (eds Fraser, N. & Sues, H.-D.) 84–97 (Cambridge Univ. Press, New York, 1994).
12. Ague, J. J., Carpenter, K. & Ostrom, J. H. Solution to the *Hallopus* enigma? *Am. J. Sci.* **295**, 1–17 (1995).
13. Clark, J.M. & Xu, X. Dinosaurs from Xinjiang, China ⟨http://www.gwu.edu/~clade/faculty/clark/china.html⟩ (2001–2003).
14. Brochu, C. A. Closure of neurocentral sutures during crocodylian ontogeny: implications for maturity assessment in fossil archosaurs. *J. Vert. Paleontol.* **16**, 49–62 (1996).
15. Jenkins, F. A. Jr The evolution of the avian shoulder joint. *Am. J. Sci. A* **293**, 253–267 (1993).
16. Müller, G. & Alberch, P. Ontogeny of the limb skeleton in *Alligator mississippiensis*: developmental invariance and change in the evolution of archosaur limbs. *J. Morphol.* **203**, 151–164 (1990).
17. Hildebr, M. & Goslow, G. *Analysis of Vertebrate Structure* (Wiley, New York, 2001).
18. Eberth, D. A. *et al.* Sequence stratigraphy, paleoclimate patterns and vertebrate fossil distributions in Jurassic–Cretaceous strata of the Junggar Basin, Xinjiang Autonomous Region, PR China. *Can. J. Earth Sci.* **38**, 1627–1644 (2001).
19. Chen, P. J. in *The Continental Jurassic* (ed. Morales, M.) 395–412 (Museum of Northern Arizona Bulletin 60, Flagstaff, 1996).
20. Lucas, S. G. *Chinese Fossil Vertebrates* (Columbia Univ. Press, New York, 2001).
21. Benton, M. J. & Walker, A. D. *Erpetosuchus*, a crocodile-like basal archosaur from the Late Triassic of Elgin, Scotland. *Zool. J. Linn. Soc.* **136**, 25–47 (2002).
22. Osmólska, H., Hua, S. & Buffetaut, E. *Gobiosuchus kielanae* (Protosuchia) from the Late Cretaceous of Mongolia: anatomy and relationships. *Acta Palaeontol. Pol.* **42**, 257–289 (1997).
23. Swofford, D. L. PAUP*Beta 10 Software (Sinauer Associates, Sunderland, Massachusetts, 2003).

**Supplementary Information** accompanies the paper on **www.nature.com/nature**.

......................................................................

# Cooperation and competition in pathogenic bacteria

**Ashleigh S. Griffin**[1], **Stuart A. West**[1] & **Angus Buckling**[2]

[1]*Institute of Cell, Animal & Population Biology, University of Edinburgh, King's Buildings, West Mains Road, Edinburgh EH9 3JT, UK*
[2]*Department of Biology and Biochemistry, University of Bath, Bath BA2 7AY, UK*

......................................................................

**Explaining altruistic cooperation is one of the greatest challenges for evolutionary biology[1–3]. One solution to this problem is if costly cooperative behaviours are directed towards relatives[4,5]. This idea of kin selection has been hugely influential and applied widely from microorganisms to vertebrates[2–10]. However, a problem arises if there is local competition for resources, because this leads to competition between relatives, reducing selection for cooperation[3,11–14]. Here we use an experimental evolution approach to test the effect of the scale of competition, and how it interacts with relatedness. The cooperative trait that we examine is the production of siderophores, iron-scavenging agents, in the pathogenic bacterium *Pseudomonas aeruginosa*[15–17]. As expected, our results show that higher levels of cooperative siderophore production evolve in the higher relatedness treatments. However, our results also show that more local competition selects for lower levels of siderophore production and that there is a significant interaction between relatedness and the scale of competition, with relatedness having less effect when the scale of competition is more local. More generally, the scale of competition is likely to be of particular importance for the evolution of cooperation in microorganisms, and also the virulence of pathogenic microorganisms, because cooperative traits such as siderophore production have an important role in determining virulence[6,9,17–19].**

Explaining altruistic cooperation is fundamental to understanding the main evolutionary transitions from single-celled organisms to complex animal societies[1]. The problem is why should an individual carry out an altruistic behaviour that is costly to perform, but benefits another individual or the local group? Hamilton's[4,5] kin selection theory provides an explanation for altruism between relatives: by helping a close relative reproduce, an individual is still passing on its genes to the next generation indirectly. This is encapsulated by Hamilton's rule[3,4], which states that an altruistic behaviour is favoured whenever $rb-c > 0$, where $r$ is the genetic relatedness between the actor and the beneficiary, $b$ is the benefit of receiving the altruistic behaviour and $c$ is the cost of performing the behaviour. The theory of kin selection is well accepted, and variation in relatedness has been applied to explain variation in the level of altruistic cooperative behaviours in organisms ranging from microorganisms to vertebrates[2–10].

However, selection for altruism depends also upon the scale of competition (population demography or structure)[3,11]. There is a